A 55 kW Three-Phase Inverter with Si IGBTs and SiC Schottky Diodes

Burak Ozpineci[1], Madhu S. Chinthavali[2], Leon M. Tolbert[1,3], Avinash Kashyap[4], and H. Alan Mantooth[4]

[1]Oak Ridge National Laboratory, Oak Ridge, TN 37831-6472 USA

[2]Oak Ridge Institute for Science and Education, Oak Ridge, TN 37831-0117 USA

[3]The University of Tennessee, Dept. of Electrical and Computer Engineering, Knoxville, TN 37996 USA

[4]University of Arkansas, Department of Electrical Engineering, Fayetteville, AR 72701 USA

***Abstract*- Silicon carbide (SiC) power devices are expected to have an impact on power converter efficiency, weight, volume, and reliability. Presently, only SiC Schottky diodes are commercially available at relatively low current ratings. Oak Ridge National Laboratory has collaborated with Cree and Semikron to build a Si IGBT– SiC Schottky diode hybrid 55kW inverter by replacing the Si pn diodes in Semikron's automotive inverter with Cree's made-to-order higher current SiC Schottky diodes. This paper presents the developed models of these diodes for circuit simulators, shows inverter test results, and compares the results to those of a similar all–Si inverter.**

I. Introduction

There is a growing demand for more efficient, higher power density, and higher temperature operation of the power converters in transportation applications. In spite of the advanced technology, silicon (Si) power devices cannot meet some transportation requirements. Silicon carbide (SiC) has been identified as a material with the potential to replace Si devices in the near term because of its superior material advantages such as wider bandgap, higher thermal conductivity, and higher critical breakdown field strength. SiC devices are capable of operating at high voltages, high frequencies, and at higher junction temperatures. Significant reduction in weight and size of SiC power converters with an increase in the efficiency is projected [1-5]. SiC unipolar devices such as Schottky diodes, VJFETs, MOSFETs, etc. have much higher breakdown voltages compared to their Si counterparts which makes them suitable for use in traction drives replacing Si pn diodes and IGBTs [6-14].

Presently, SiC Schottky diodes are the most mature and the only commercially marketed SiC devices available. These diodes are commercially available up to 1200V/20A or 600V/20A.

SiC Schottky diodes have been proven to have better performance characteristics when compared to their equivalent Si pn diodes [1], especially with respect to the switching characteristics. SiC devices can also operate at higher temperatures and thereby resulting in reduced heatsink volume.

It is expected that the first impact of SiC power devices on automotive traction drives will be observed when SiC Schottky diodes replace Si pn diodes in inverters. Oak Ridge National Laboratory (ORNL) has collaborated with Cree and Semikron to build a Si IGBT– SiC Schottky diode hybrid 55kW inverter by replacing the Si pn diodes in Semikron's automotive inverter with Cree's SiC Schottky diodes. This paper shows the results obtained from testing this inverter and comparing it to a similar all–Si inverter.

II. SiC Schottky Diodes

Semikron has built 55kW Automotive Integrated Power Modules (AIPM) for the U.S. Department of Energy's FreedomCAR Program's hybrid electric vehicle traction drives. These modules contain three-phase inverters with 600V/600A Si IGBTs and pn diodes.

For an ORNL project, Cree has developed 600 V/75 A SiC Schottky diodes as shown in Fig. 1. Semikron has replaced each Si pn diode in their AIPM with two of these 75A SiC Schottky diodes.

A. Static Characteristics

After extensive testing, *I-V* characteristics of these diodes were obtained at different temperatures in the -50°C to 175°C ambient temperature range (Fig. 2). Considering the piece-wise linear (PWL) model of a diode, which includes a dc voltage drop, V_D and a series resistor, R_D; the diode *I-V* curves can be approximated with the following equation:

$$V_d = V_D + R_D \cdot I_d \tag{1}$$

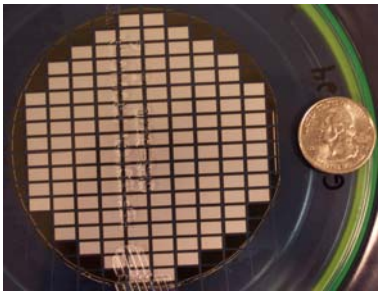

Fig. 1. The 600V/75A SiC Schottky diodes on a wafer next to a quarter.

Prepared by the Oak Ridge National Laboratory, Oak Ridge, Tennessee 37831, managed by UT-Battelle for the U.S. Department of Energy under contract DE-AC05-00OR22725.

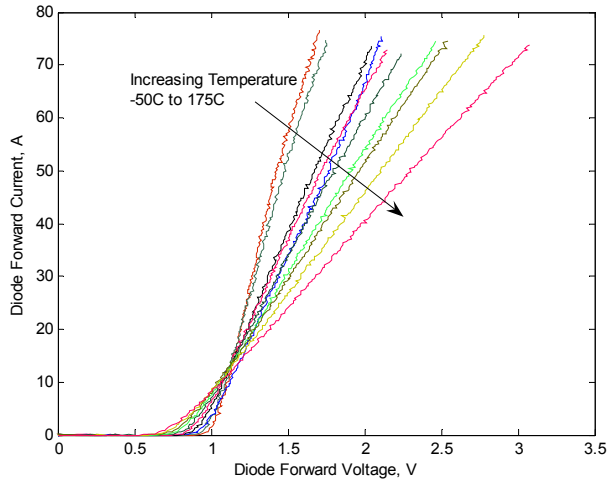

Fig. 2. Experimental I-V curves of the 75A SiC Schottky diode.

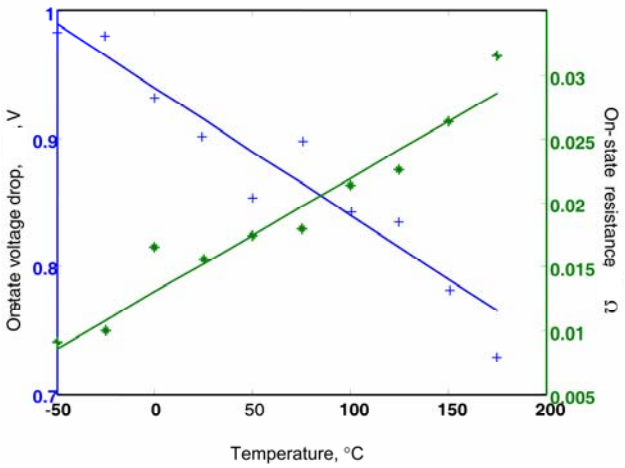

Fig. 3. R_D and V_D obtained from the experimental data in Fig.2.

where V_d and I_d are the diode forward voltage and current, and V_D and R_D are the diode PWL model parameters.

Fig. 3 shows R_D and V_D values of the 600V/75A SiC Schottky diodes with respect to temperature. As seen in these figures, V_D decreases with temperature and R_D increases with temperature. The increase in R_D indicates that the SiC Schottky diodes have a positive temperature coefficient, which implies that these devices can be paralleled easily. The equations below show the temperature dependence of the SiC Schottky diode PWL model parameters.

$$V_D = -0.001 \cdot T + 0.94 \tag{2}$$

$$R_D = 8.9 \times 10^{-5} \cdot T + 0.013 \tag{3}$$

where T is the temperature in °C.

Another model of this SiC diode has also been developed for use in circuit simulators. The model, which was constructed in MAST HDL and simulated in the Saber simulator, was based on a diode model [15] developed at the University of Arkansas. Fig. 4 shows how the static characteristics of the model fit the experimental results. The

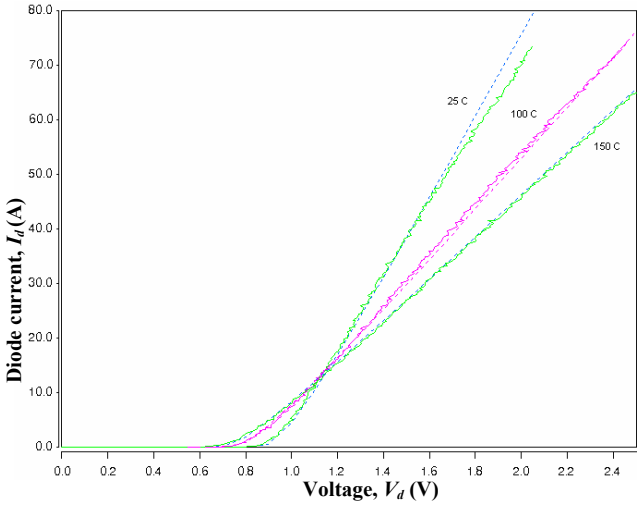

Fig. 4. Measured (solid) and simulated (dotted) on-state waveforms of the SiC Schottky diode at different temperatures.

percentage error is approximately 0.3–0.4% in the 100°C and 150°C curves and approximately 2–3% in the 25°C curve. Table I contains the values of the modeling parameters for this diode.

B. Dynamic Characteristics

The SiC Schottky diode was also tested in a chopper circuit to observe its dynamic properties. The chopper was switched at 1 kHz with a 40% duty cycle. The reverse recovery current waveforms obtained for different forward currents are shown in Fig. 5. As seen in this figure, the reverse recovery current does not change with forward current. Note that theoretically, Schottky diodes do not display reverse recovery phenomenon.

Required junction capacitance for the diode model listed in Table I is obtained from the experimental reverse recovery current waveforms. The corresponding fit of the model to the experimental waveform is shown in Fig. 6 for a forward current of 3 A. Note that the reverse recovery current is larger in this plot compared to the ones in Fig. 5. This is because the

TABLE I
SiC POWER DIODE MODEL PARAMETERS AND EXTRACTION CHARACTERISTICS FOR THE CREE 75 A DIODE

Parameter	Value
Bandgap, *EG*	1.6
Built-in junction potential, *VJ*	1.5
Zero-bias junction capacitance, *CJ*0	20×10^{-12}F
P-N grading coefficient, *M*	0.5
Forward-bias deletion capacitance coefficient, *FC*	0.5
Base doping concentration, *NB*	1×10^{15}
Forward series contact resistance, *RS*	0.013
Low-level recombination saturation current, *ISR*	5×10^{-16}
Low-level recombination emission coefficient, *NR*	1
ISR temperature exponent, *XTIR*	3
Linear NR temperature coefficient, *TNR1*	0
Quadratic NR temperature coefficient, *TNR2*	0
Linear RS temperature coefficient, *TRS1*	-14×10^{-3}
Quadratic RS temperature coefficient, *TRS2*	-16×10^{-6}
RS temperature exponent, *GAMMA*	2.5

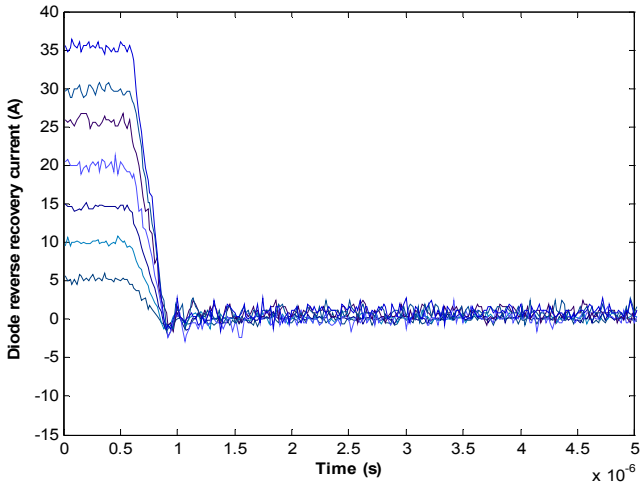

Fig. 5. Reverse recovery current waveforms of the SiC Schottky diode for different forward current values.

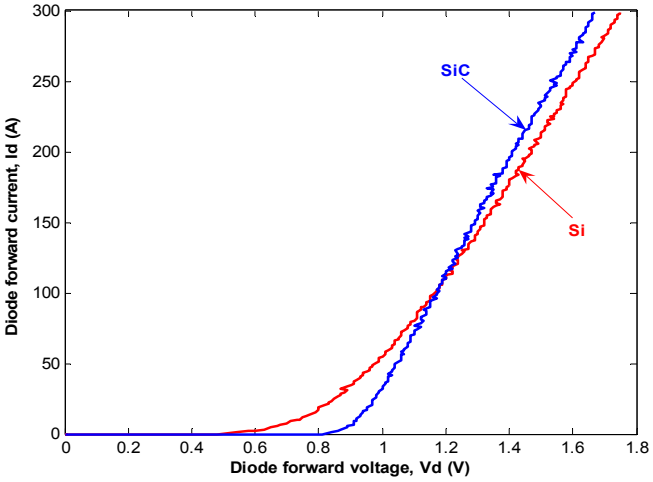

Fig. 7. The static characteristics of the packaged 600 V/ 450 A SiC Schottky and Si pn diodes at room temperature.

forward current is selected to be much smaller to observe the fit in detail.

C. Comparison with a Si pn Diode

The automotive inverter used in this study has 600 V/ 450 A diodes. For this reason, six 75 A SiC Schottky diodes are used to replace three 150 A Si pn diodes. The static characteristics of the packaged 600 V/ 450 A SiC Schottky and Si pn diodes at room temperature are shown in Fig. 7. As seen in this figure, both of the diodes have similar characteristics. At low currents, the Si pn diode has lower voltage drop while at higher currents, the SiC Schottky diode has lower voltage drop; therefore, for higher power operation, SiC Schottky diodes will have lower conduction losses.

Switching losses of the 75 A SiC Schottky diode have been shown in Fig. 5. Similar tests have been done on the 150 A Si pn diodes. The results of these tests can be seen in Fig. 8. It can be observed that the peak reverse recovery current of the Si pn diode is much higher than that of the SiC Schottky diode at the same forward current and increases further with increasing forward current. This corresponds to high reverse recovery losses that increase with forward current. Fig. 9 shows the comparison of the energy losses per turn-off of a 75A SiC Schottky diode and a 150V Si pn diode. As the diode forward current increases, the energy losses of the Si pn diode increase exponentially while those of the SiC Schottky diode are negligible.

As a summary, the static characteristics of both of the tested diodes are similar; however, the dynamic characteristics are much different. Si pn diode has high peak reverse recovery currents that result in high diode switching losses and extra IGBT losses since the reverse current has to go through a main switch. Consequently, it is expected for the Si IGBT– SiC Schottky diode inverter to perform better than the similar all–Si inverter.

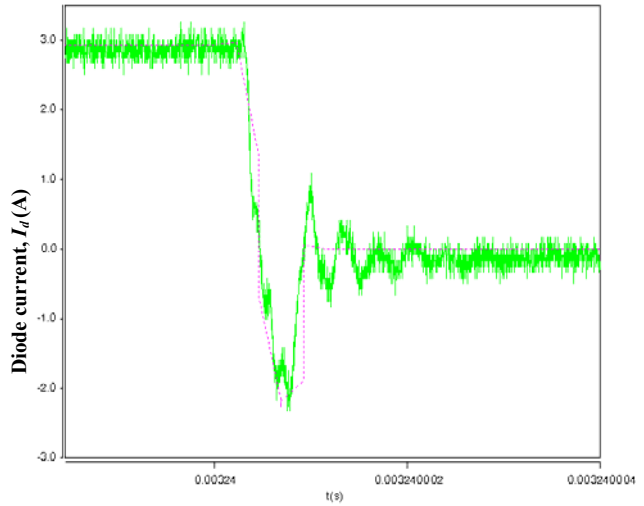

Fig. 6. Measured (solid) and simulated (dotted) reverse-recovery waveforms of the SiC Schottky diode.

III. Inductive Load Test

Both the Si–SiC hybrid and the all–Si inverters were tested with an inductive load and a dyne set with the same procedure and the same conditions.

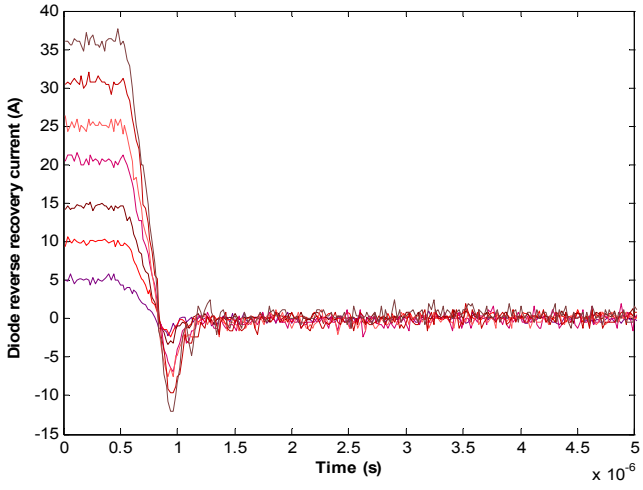

Fig. 8. Reverse recovery current waveforms of the SiC Schottky diode for different forward current values.

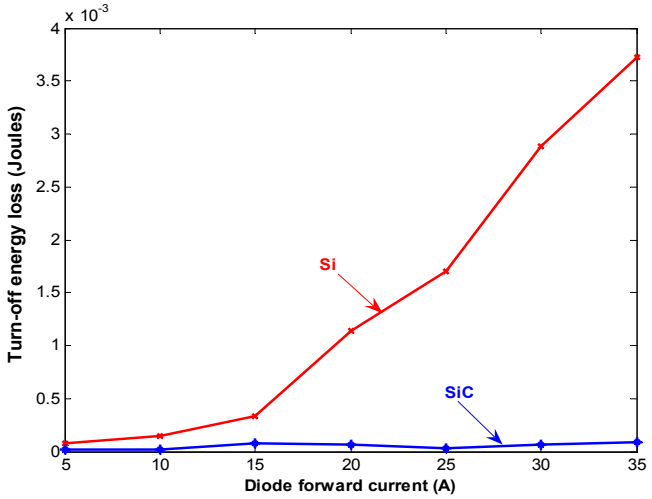

Fig. 9. The experimental turn-off energy losses of a 75 A SiC Schottky diode and a 150 A Si pn diode at room temperature.

For the inductive load test, the output leads of the inverter are connected to a three-phase star connected variable resistor bank with a three phase inductor in series. The dc inputs are connected to a voltage source capable of supplying the maximum rated operating voltage and current levels for the inverter. The test setup is shown in Fig. 10.

The dc link voltage was varied from the minimum operating voltage of 200 V to the maximum bus voltage of 450 V.

The load resistance was set to the minimum value and the output current was varied. The inverter was operated with a 20°C coolant at a flow rate of 9.46 liters per minute. The open loop frequency of operation and the PWM frequency (10 kHz) were fixed and the current command was varied for a particular dc link voltage. For each value of the current command and open loop frequency, the dc link voltage, dc link current, input/output power, efficiency, and output line currents and voltages were recorded. The three-phase power was measured using the two wattmeter method.

The command current was increased in steps of 10 A without exceeding the power rating of the inverter or the power rating of the load. The procedure was repeated by

Fig. 10. Inductive load test set-up.

increasing the open loop frequency in steps of 25 Hz.

The coolant temperature was changed to 70ºC and the above procedure was repeated to observe the operation at higher temperatures.

The operating waveforms, for two specific operating conditions of the Si–SiC hybrid inverter are shown in Fig. 11.

The data obtained for both of the inverters were analyzed, and the corresponding efficiencies were calculated. The efficiency versus output power plots for several operating conditions are shown in Fig. 12.

The average loss reduction resulted in using SiC Schottky diodes instead of Si pn diodes was calculated as:

$$\%\,loss\ reduction = \frac{P_{loss}^{Si} - P_{loss}^{SiC}}{P_{loss}^{Si}} \times 100\,. \qquad (4)$$

The Si–SiC hybrid inverter losses are up to 33.6% less than the all–Si inverter.

IV. Dynamometer Test

The inverters were connected individually to an induction machine set up in a dynamometer test cell to test them for their dynamic performance in the motoring and regeneration modes. The induction motor used was a four-pole induction motor with a base speed of 2500 rpm and the dynamometer had 100-hp capacity. The tests were performed

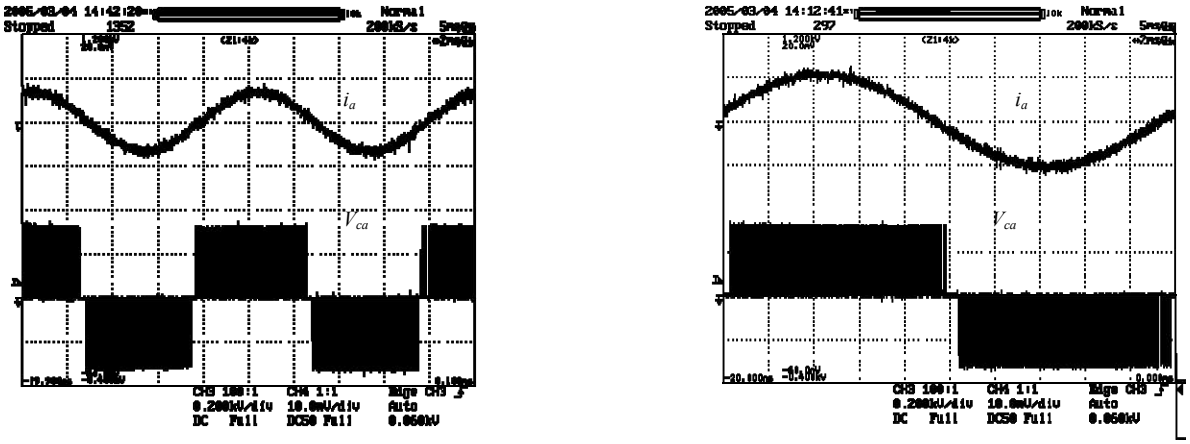

(a) V_{dc}=325V; $i_{a,peak}$= 80A; f_o=50Hz

(b) V_{dc}=325V; $i_{a,peak}$= 60A; f_o=100Hz

Fig. 11. Inverter output voltage and current during the inductive load test for two different conditions.

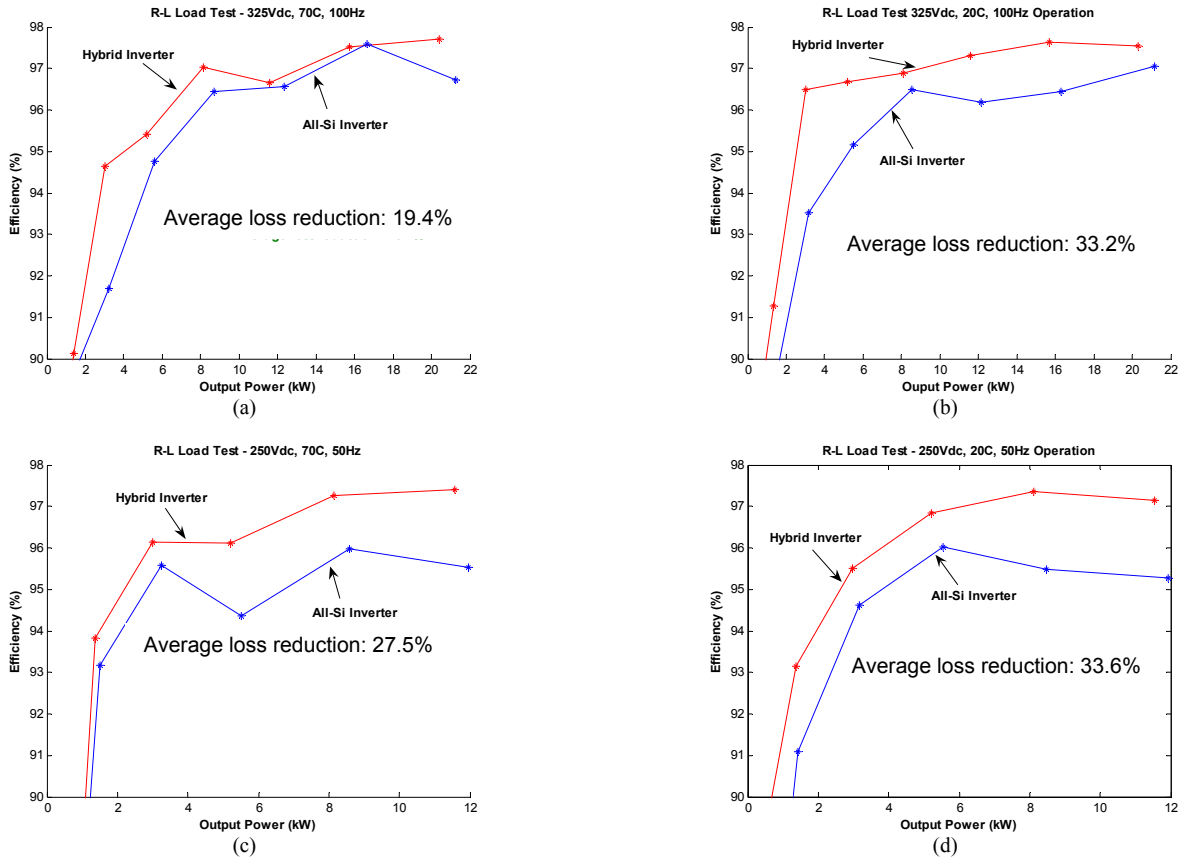

Fig. 12. R-L load test efficiency curves for various load conditions.

with the inverter being supplied with 70ºC coolant and a flow rate of 9.46 liters per minute.

A. Motoring Mode

In this mode, the speed set point, the magnetizing current, the direction of rotation, and the current limit were the parameters that could be adjusted. The dc voltage input to the inverter was set at the nominal battery operating voltage (325 Vdc). The closed loop speed controller gains were adjusted for a given magnetizing current value and current limit to achieve a stable operation of the system for wide range of speeds. The direction of rotation was set to forward and the motor speed was increased from 750 rpm to the rated base speed for a specific continuous load torque. The load torque was varied gradually from zero to the required torque and then decreased to zero. The data was obtained for a wide range of speed and torque values by changing the load torque (100, 150, 200 Nm) using the dynamometer controller. The following information was recorded at each speed increment: motor shaft speed, motor torque, input and output voltages, and currents.

The operation waveforms for two different load conditions are shown in Fig. 13. The efficiency plots for various speed and load torque are shown in Fig. 14. The average loss reduction was obtained as described in the previous section. In this case, up to 10.7% reduction in the losses is observed.

B. Regeneration Mode

In this mode, the torque limit and the operating current can be adjusted. The dc voltage input to the inverter was set at the nominal battery operating voltage. The direction of rotation was set to be forward. The dynamometer controller was adjusted to control the speed while the inverter controller controlled the current. Data has been collected for 100, 150, and 200 Nm torque produced by the drive.

The procedure was repeated to obtain the data for a wide range of speed and torque values. The following information was recorded at each speed increment: motor shaft speed, motor torque, input and output voltages and currents.

The operating waveforms for the regeneration mode are shown at two different speeds in Fig. 15. The curves comparing the efficiency of the inverters at 70ºC are shown in Fig. 16. In this mode, the reduction in the losses is comparable to the motoring case.

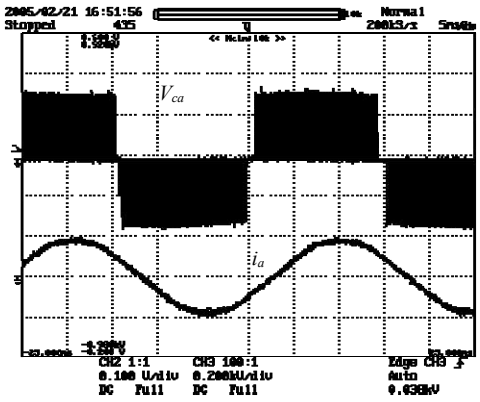

(a) 1000 rpm and 50 Nm

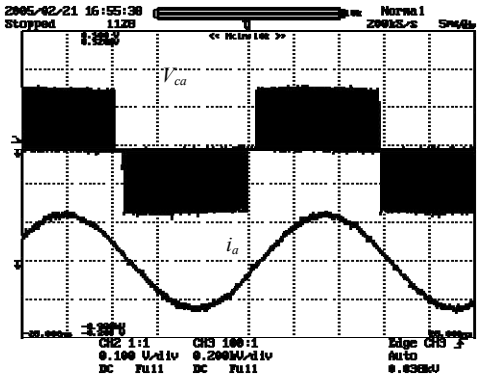

(b) 1000 rpm and 150 Nm

Fig. 13. Inverter output voltage and current during the dyne test for two different conditions.

V. Conclusions

The testing of both the Si–SiC hybrid and all-Si inverters was completed successfully. The inverters were able to operate at peak power levels with efficiencies greater than 90%. The inverters were tested for a peak power of 47 kW and continuous rating of up to 35 kW.

The test results show that by merely replacing Si pn diodes with their SiC Schottky diode counterparts, the losses of an inverter decrease considerably. As the device tests showed, the main reason for this is the high reverse recovery losses of Si pn diodes which are negligible for SiC Schottky diodes.

Note that both of the inverters were tested in the exact same conditions with the same controller. Since SiC Schottky diodes have negligible reverse recovery, they do not stress the main switches as much as Si pn diodes. Therefore, it is possible to operate the Si–SiC hybrid inverter at higher switching frequencies than the one used in these tests.

Acknowledgment

The authors would like to thank Drs. Anant Agarwal and Sei-Hyung Ryu of Cree and Dr. John Mookken of Semikron for their part in building the hybrid inverter.

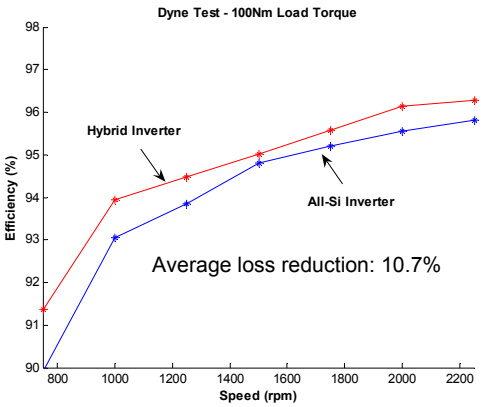

(a) 100 Nm

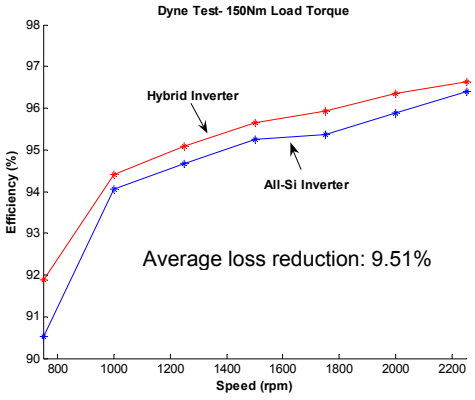

(b) 150 Nm

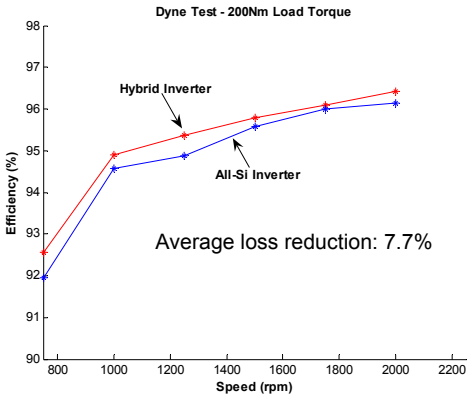

(c) 200 Nm

Fig. 14. Dynamometer test – motoring mode efficiency plots at 70ºC with a) 100 Nm, b) 150 Nm, c) 200 Nm, load torques.

References

[1] B. Ozpineci, L. M. Tolbert, S. K. Islam, F. Z. Peng, "Testing, characterization, and modeling of SiC diodes for transportation applications," *IEEE Power Electronics Specialists Conference*, June 23–27, 2002, Cairns, Australia, pp. 1673–1678.

[2] L. M. Tolbert, B. Ozpineci, S. K. Islam F. Z. Peng, "Impact of SiC power electronic devices for hybrid electric vehicles," *2002 Future Car Congress Proceedings*, June 3–5, 2002, Arlington, Virginia. (SAE paper number 2002–01–1904).

[3] http://powerelectronics.com/mag/408pet20_web.pdf.

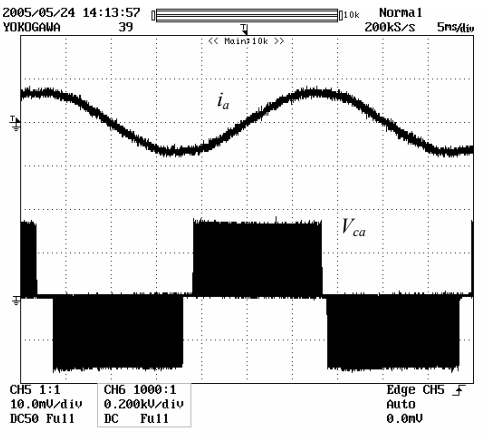

(a) 1000 rpm and 50 Nm

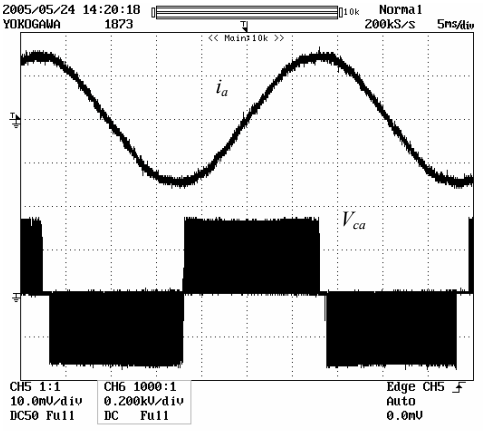

(b) 1000 rpm and 150 Nm

Fig. 15. Inverter output voltage and current during the regeneration test for two different conditions.

[4] H. R. Chang, E. Hanna, A. V. Radun, "Demonstration of silicon carbide (SiC) – based motor drive," *Conference of the IEEE Industrial Electronics Society*, vol. 2, 2–6 November 2003, pp. 1116 – 1121.

[5] Abou-Alfotouh, A. M. Radun, V. Arthur, H. R. Chang, C. Winerhalter, "A 1 MHz hard-switched silicon carbide DC/DC converter," *IEEE Applied Power Electronics Conference*, 9-13 Feb. 2003, pp. 132 – 138.

[6] K. Mino, K. S. Herold, J. W. Kolar, "A gate drive circuit for silicon carbide JFET," *Conference of the IEEE Industrial Electronics Society*, vol. 2, 2–6 November 2003, pp. 1162 – 1166.

[7] M. L. Heldwein, J. W. Kolar, "A novel SiC J-FET gate drive circuit for sparse matrix converter applications," *IEEE Applied Power Electronics Conference*, vol. 1, 22–26 February 2004, pp. 116 – 121.

[8] M. Bhatnagar, P. K. McLarty, B. J. Baliga, "Silicon carbide high voltage (400V) Schottky barrier diodes," *IEEE Electron Device Letters*, vol. 13, no. 10, October 1992, pp. 501–503.

[9] A. R. Hefner, R. Singh, J. Lai, D. W. Berning, S. Bouche, C. Chapuy, "SiC power diodes provide breakthrough performance for a wide range of applications," *IEEE Transactions on Power Electronics*, vol. 16, no. 2, March 2001, pp. 273–280.

[10] B. Allebrand, H. Nee, "On the possibility to use SiC JFETs in power electronic circuits," *European Conference on Power Electronics and Applications,* Austria, 2001.

[11] M. Ruff, H. Mitlehner, R. Helbig, "SiC devices: Physics and numerical simulation," *IEEE Transactions on Electron Devices*, vol. 41, no. 6, June 1994, pp. 1040–1054.

[12] D. Peters, H. Mitlehner, R. Elpelt, R. Schorner, D. Stephani, "State of the art technological challenges of SiC power MOSFETs designed for high blocking voltages," *European Conference on Power Electronics and Applications*, 2-4 September 2003, Toulouse, France.

[13] S. H. Ryu, A. Agarwal, J. Richmond, J. Palmour, N. Saks, J. Williams, "10A, 2.4kV power DIMOSFETs in 4H-SiC," *IEEE Electron Device Letters*, vol. 23, no. 6, June 2002, pp. 321–323.

[14] S. H. Ryu, S. Krishnaswami, M. Das, J. Richmond, A. Agarwal, J. Palmour, J. Scofield, "4H-SiC DMOSFETs for high speed switching applications," *5th European Conference on Silicon Carbide Related Materials*, August 31- September 4, 2004.

[15] T. R. McNutt, "Modeling and Characterization of Silicon Carbide Power Devices," *Ph.D. Dissertation*, Department of Electrical Engineering, University of Arkansas, Fayetteville, Arkansas, 2004.

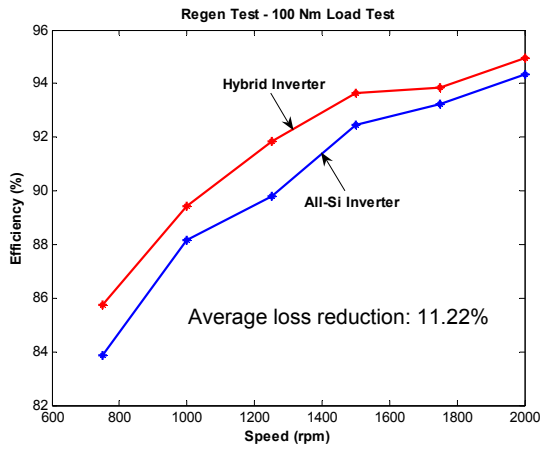

(a) 100 Nm

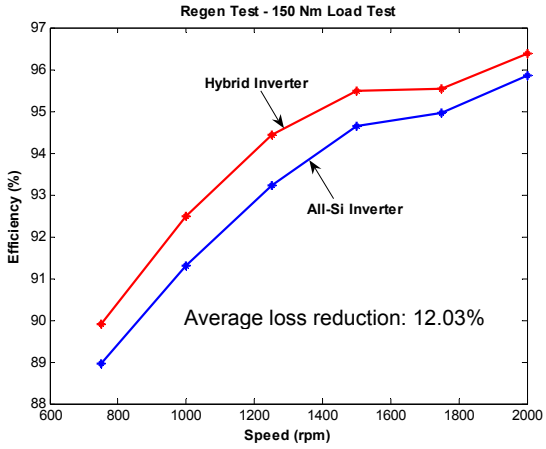

(b) 150 Nm

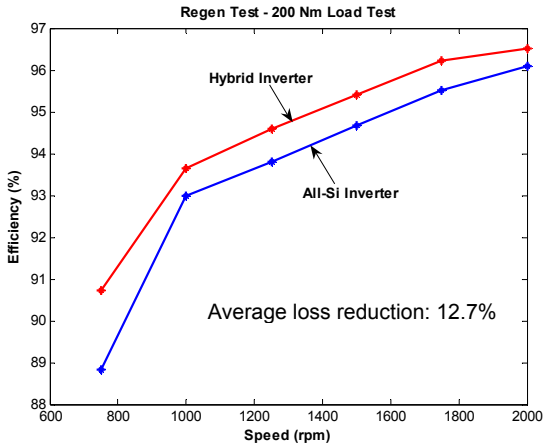

(c) 200 Nm

Fig. 16. Dynamometer test –regeneration mode efficiency plots at 70ºC with a) 100 Nm, b) 150 Nm, c) 200 Nm load torques.